Measuring Influenza A surface protein activity using OI-RD detection

M. R. Warner, J. P. Landry, Y. Y. Fei, D. D. Hernandez, D. Allison, and X. D. Zhu

Abstract

In this paper, we use OI-RD microscopy techniques to investigate the surface protein activity of different strains of Influenza A virus in order to elucidate a binding profile for the different strains, four pandemic and one seasonal. Influenza A has two main surface proteins, Hemagglutinin (HA) that attaches and Neuraminidase (NA) that removes the virus from the host cell. We used OI-RD techniques to view activity of the two proteins with different glycans, including differentiating between α 2-3 sialated glycans and α 2-6 sialated glycans. We found that seasonal virus bound to α 2-6 but also α 2-3, an unexpected result. We witnessed NA activity but further research is required.

Introduction

Influenza A virus particles invade host cells by first binding at the cell surface. The surface of the virus is coated with two glycoproteins, hemagglutinin (HA) and neuraminidase (NA), which function to, respectively, attach to and release from host cells (1). There are about 400 Hemagglutinin proteins on a typical virus that attach to host cells by binding to many sialylated glycans (2). Much research has gone into finding ways to block this HA activity and understand what exactly the HA can bind to. In this paper, we will explore the binding profile of different strains of influenza A to a set of different glycans.

A somewhat less explored activity is that performed by neuraminidase, of which there are about 100 proteins for the average virus. NA functions to cleave the sialic acid

and the virus from the host cell, both when it is exiting the cell after replication and when it is trying to bind (3). As one might expect, it has been found that optimal ratios exist for HA: NA to achieve the correct amout of association and dissociation.

Earlier research has looked into quantifying NA activity by using peroxide-conjugated peanut agglutinin (Po-PNA) (4). The basic methodology is this: Coat sialylated glycans, some of which PNA can bind to their base structures, and coat with neuraminidase. PNA was then pipetted in and bound to formerly sialylated sugars where NA activity had occurred.

In this paper we will use the optical method Oblique-Incidence Reflectivity Difference (OI-RD) to try to ascertain different strains' NA activity and profile. OI-RD is a label-free detection method that has shown the ability to detect biomolecular arrays and take both endpoint and real-time data of many parallel reactions in microarrays (5, 6). We will use this ability to perform assays with different strains and PNA binding to 24 glycans.

Methods

Experimental Apparatus

Figure 1 shows a schematic of our experimental device. As previously explained (7), the laser emits light at a wavelength of 632.8 nm. The light passes through a photo-elastic modulator, which causes the p and s-components of the light to oscillate with a frequency of 50 kHz. The light passes through a phase shifter, which induces an adjustable phase difference between the two polarized states. The beam is reflected off the glass surface and through an objective lens, which focuses the light into the photodiode.

The signal is then received by two lock-ins which perform fourier decomposition on the two analog signals. The fourier decomposition results in amplitudes for the first and

second harmonics of the light. These amplitudes are then used to form images and real-time curves on the program *Scan Controller*, written by J.P. Landry in LabView. Our system is aligned so that the first harmonic corresponds to the phase difference (imaginary part) of the differential perturbation of the two components while the second corresponds to the perturbation of the real part (reflectivity change). The phase difference is relevant for small signal changes (i.e. proteins) while the reflectivity difference is relevant for large changes (i.e. virus and bacteria).

Experiment Specifics

We dispensed samples listed in Tables 1 and 2 into a 384-well plate. Using an OmniGrid 100 contract-printing arrayer (Digilab, Holliston, MA, USA), we printed four replicates each on streptavidin-coated glass slides. All sugars are biotin-conjugated (See Table 1) which adheres to the streptavidin. Samples were printed five times to increase likelihood of adherence to the slide.

HA activity

Earlier unpublished research by Y. Y. Fei (see Table 3) revealed a binding profile, signifying HA activity for four pandemic and one seasonal strain. Seasonal strain grown in egg had not yet been tested so we received sample of MDCK-1, MDCK-2, and seasonal grown in egg to test all at the same time. To run the virus experiments, we first 'blocked the slide' with 7600 nM biotion-conjugated BSA so that the virus would not bind to the slide. We then imaged, flowed 5000 HAU/mL virus in, delayed for six hours to allow association, and flushed with PBS and allowed two hours for dissociation. We then imaged again and took the difference image to see where the viruses bound to.

NA activity

As described earlier, we had reason to believe that after NA activity occurred from the viruses, PNA may be able to bind to glycans that had their sialic acid clipped. To test the binding profile of PNA, we first blocked again with BBSA and imaged. We then replaced the fluid in the chamber with 9000 nM PNA, waited one hour, and imaged again before flushing. We then flushed, waited an hour, and imaged.

After establishing PNA's profile, we continued by again blocking the slide and flowing in 5000 HAU/mL virus and waited two hours. We then flushed the virus and added PNA, waited 1.5 hours, and imaged. We repeated with all four viruses, eventually dropping concentration to 1000 HAU/mL and dropping exposure time of virus to 1 hr. to attempt to avoid saturation.

Results/Discussion

HA activity

MDCK-1 bound to α 2-6 glycans OS 21-24 and more lightly to α 2-3 glycans OS 12-14 (see fig.2). MDCK-2 bound to α 2-6 glycans OS 21-24 and more lightly to α 2-3 glycans OS 12-14 (fig. 3). The seasonal virus grown in egg bound to α 2-6 glycans OS 21-24 and lightly to OS-14 (fig. 4). These results differed from past results achieved with the same microscope in which MDCK-1 showed no α 2-3 binding and MDCK-2 bound only to OS-14 (Table 3). A few possibilities exist for this discrepancy. It is possible that since the signal from α 2-6 glycans was so strong originally compared to OS-13 and OS-14, for example, that α 2-3 binding was disregarded as non-specific binding. It is also remotely possible that the virus could have somehow changed during storage at 4° C, though this seems unlikely.

NA activity

PNA flowed by itself bound to OS-03 and OS-09 strongly and OS-01 and OS-07 more lightly (fig. 5). The latter binding was somewhat more temporary—after PBS washing it disappeared. PNA also bound to one spot on OS-08 strongly. Previous research showed PNA's binding profile to contain only 01 and 09 because only endpoint study was done (8). The spot on OS-08 was likely contaminated—we did not see this pattern in any other experiments, just the consistent binding to OS-09, 01, 03, and 07.

While many other virus-PNA assays were performed, the only two pandemic assays that showed results of PNA binding were PR8 and Phillipines. Concentrations of viruses where 5000 HAU/mL. Delay after flowing in virus was 2 hrs, with a 30 minute dissociation time after PBS was flowed. PNA was allowed to associate for 1.5 hours and dissociate for 30 minutes. An image was taken before dissociation that showed binding in both virus experiments to OS-21 and OS-17, which correspond to OS-03 and OS-09 respectively (figs 6 and 7).

We had been trying to reduce concentration and change association time with udorn and Mem71 and never did see PNA activity, but this was likely because time ran short and only so many experiments could be done. We had been expecting to see binding to more glycans that corresponded to PNA's binding profile. It is possible that the glycans were saturated to the point that PNA could not bind. The dissociation time likely was not long enough for the virus, not giving enough time for the NA to clip the sialic tail. Nonetheless, this assay did show that PNA binding can indicate NA activity, which is promising for future studies regarding such activity.

Future Directions

The results show that NA activity can indeed be monitored using PNA. In the future, this experiment can be repeated with Mem71 and udorn to try to at least get as strong of a profile as that for PR8 and Philippines. Experiments should continue to be run to try to reduce the saturation to the point that the amount of NA activity measured is independent of virus concentration. When this standard point is found, assays testing NA activity in a variety of chemical conditions (pH, anti-virals, etc.) can be performed. Through all of this, an NA binding profile can be constructed for each virus. Together with the existing HA profile, this will yield a fast and accurate way to identify a strain of virus in a sample.

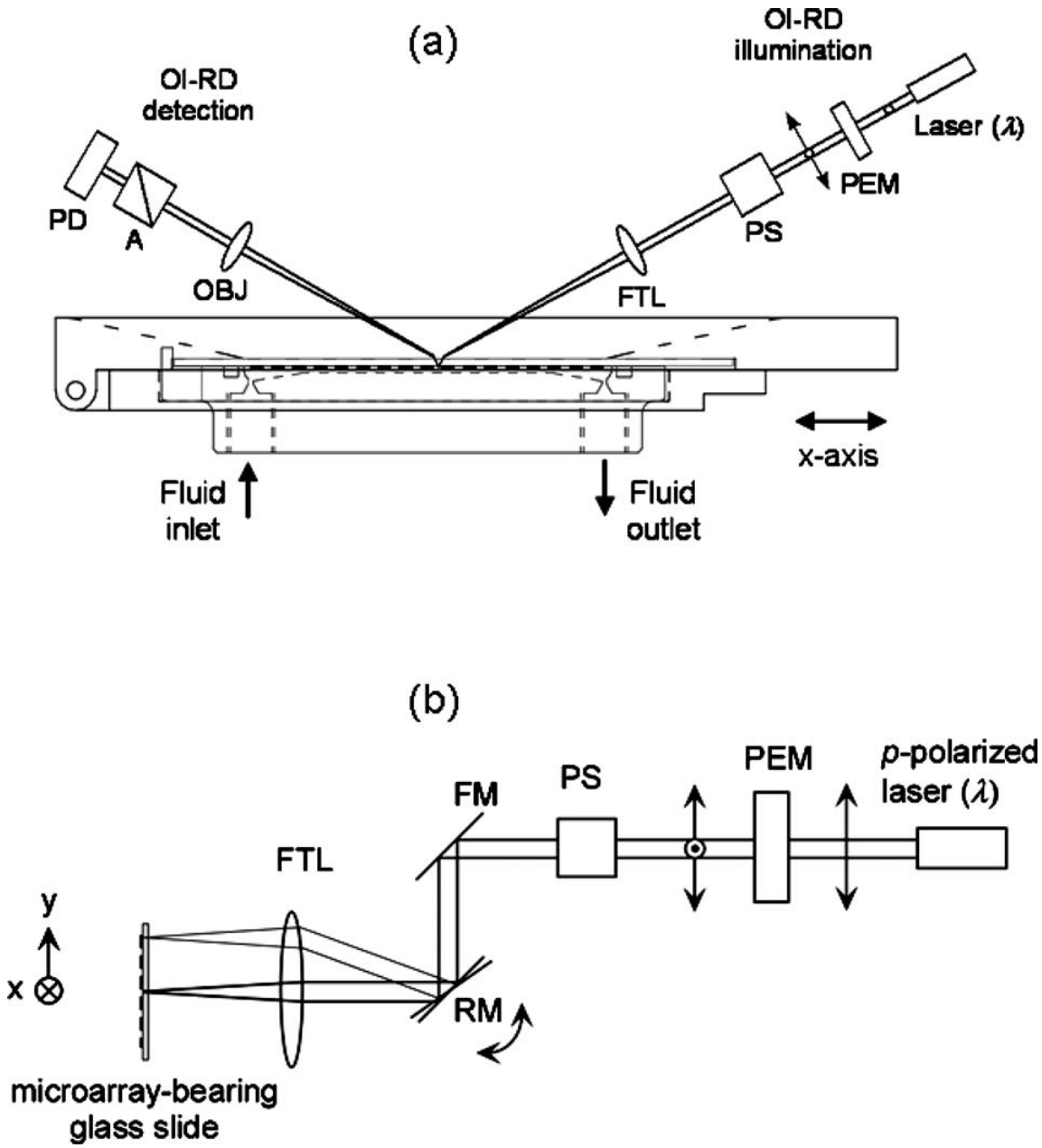

Fig. 1 a) View of microscope apparatus with both y-axis scan mirror (RM) and an x-axis translational stage. b) Side view of microscope showing functionality of the scan mirror. Figure taken from Fei et. al. 2010 (9)

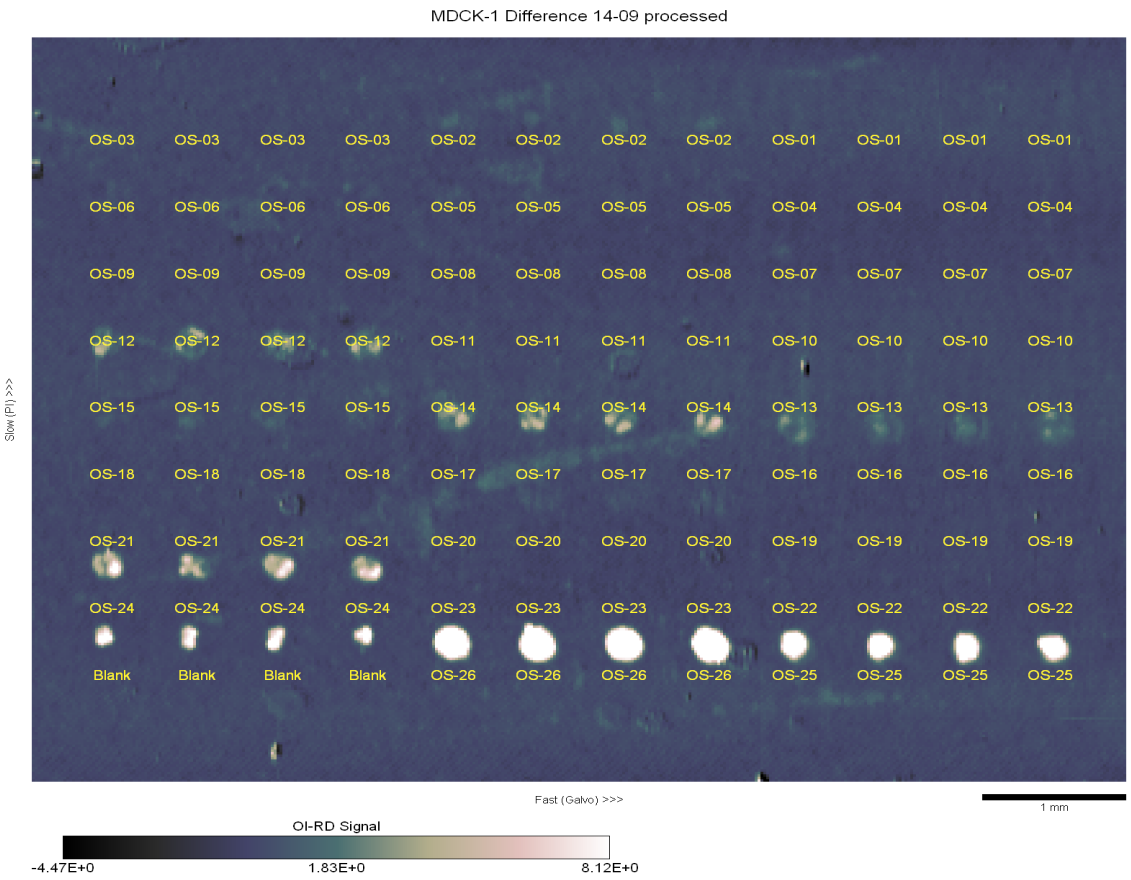

Fig.2 120808 Difference image showing binding of seasonal MDCK-1 virus, after PBS washing. Concentration 5000 HAU/mL. 6 hr. association, 2 hr. dissociation.

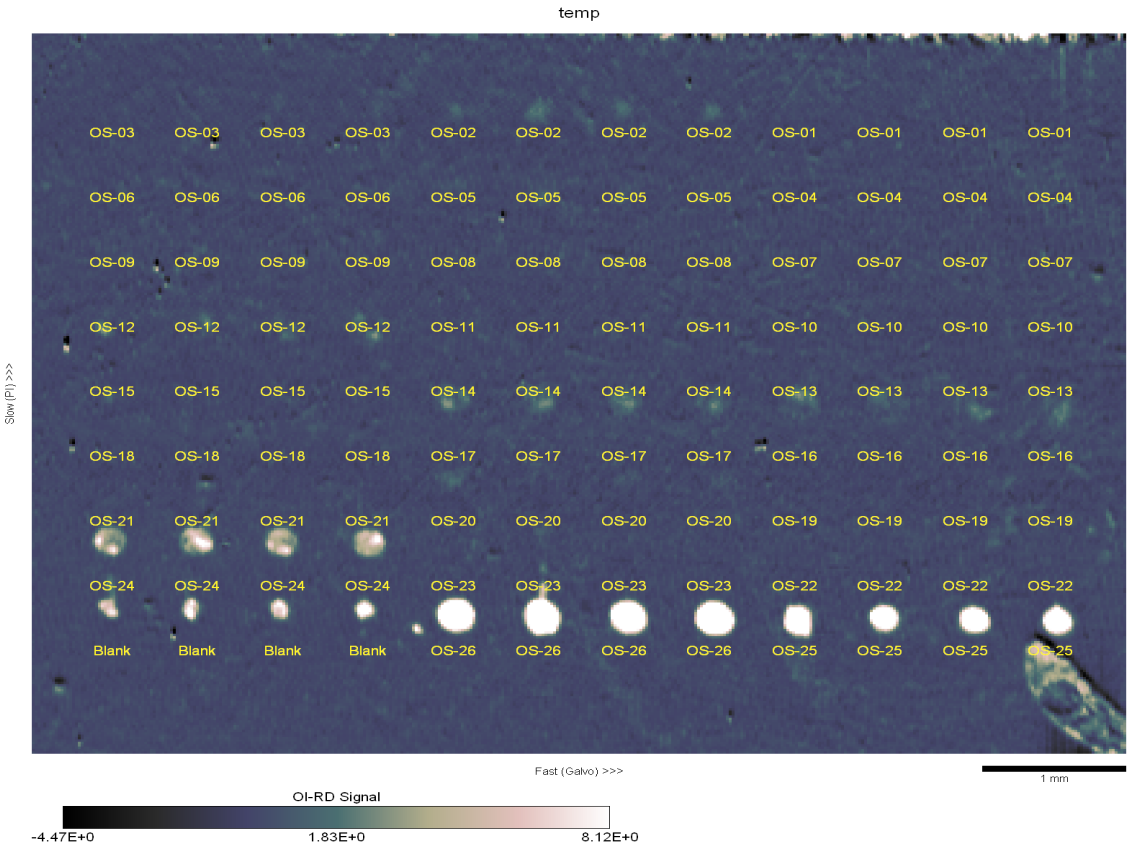

Fig. 3 120807 Difference image showing binding of seasonal MDCK-2 virus, after PBS washing. Concentration 5000 HAU/mL. 6 hr. association, 2 hr. dissociation.

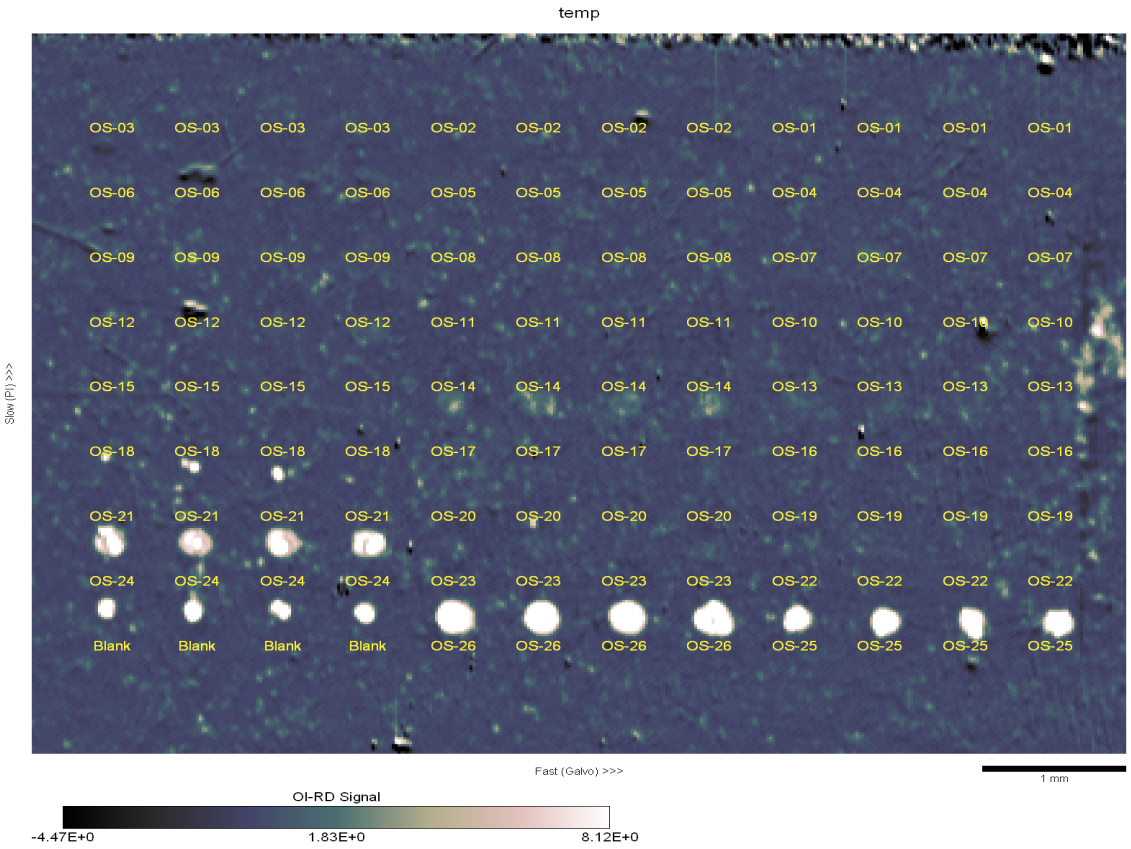

Fig. 4 120807 Difference image showing binding of seasonal egg virus, after PBS washing. Concentration 5000 HAU/mL. 6 hr. association, 2 hr. dissociation.

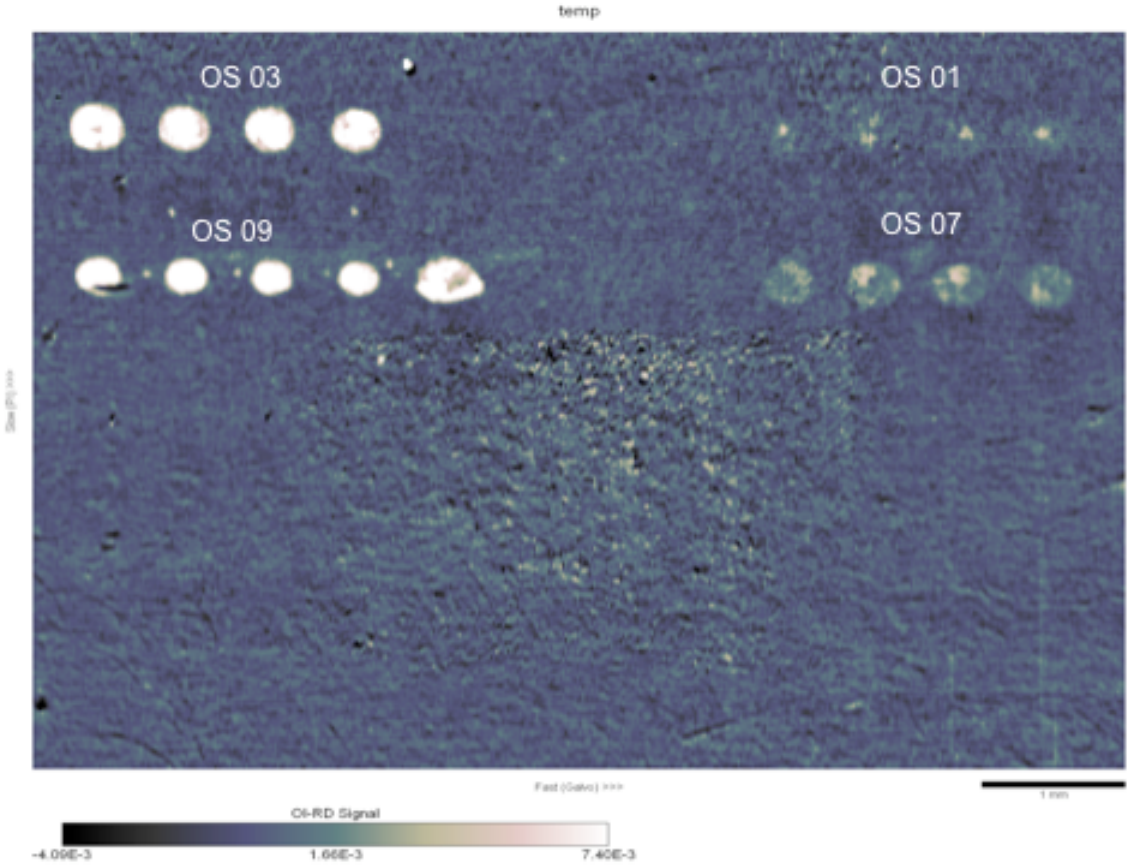

Fig. 5

120723 Difference image showing PNA binding (9000 nM, before PBS washing).

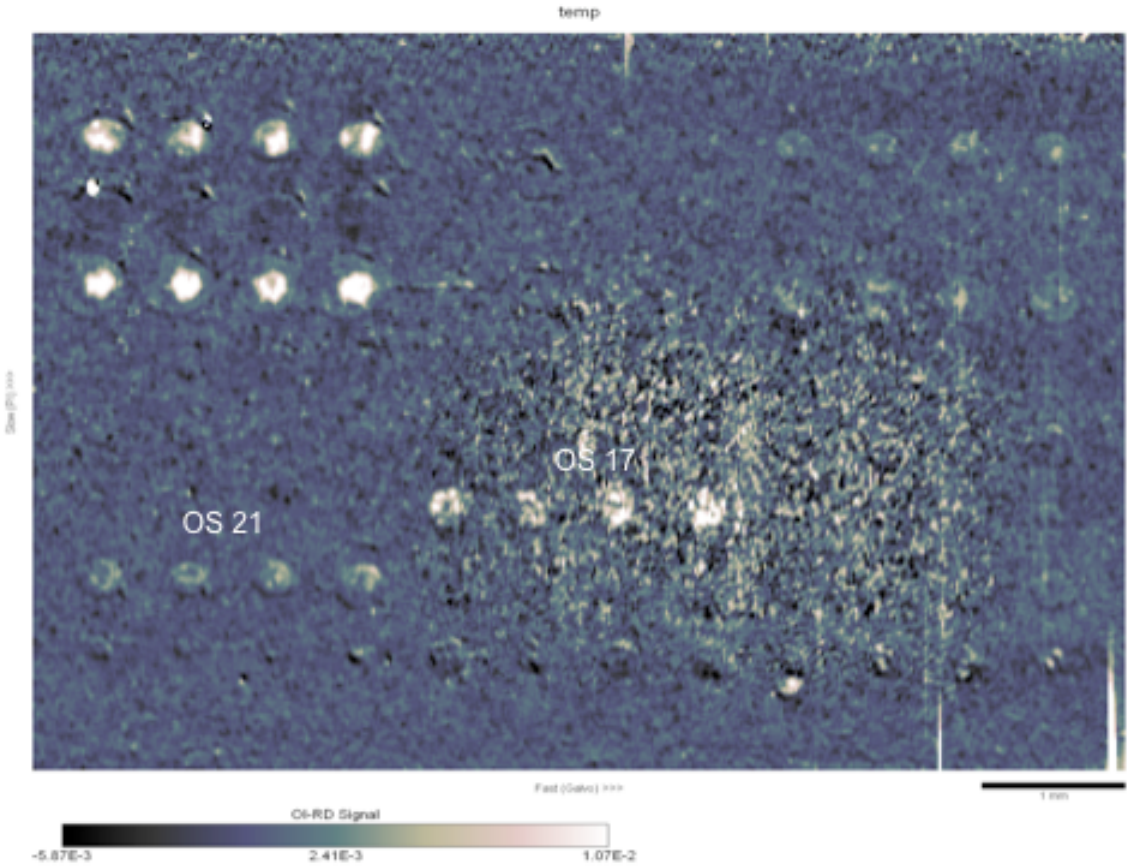

Fig. 6 120813 Difference image showing PNA (9000 nM, 1.5 hr. assoc.) binding after PR8 was flowed (5000 HAU/mL, 2 hr. assoc., .5 hr. dissoc.). Image before PBS washing.

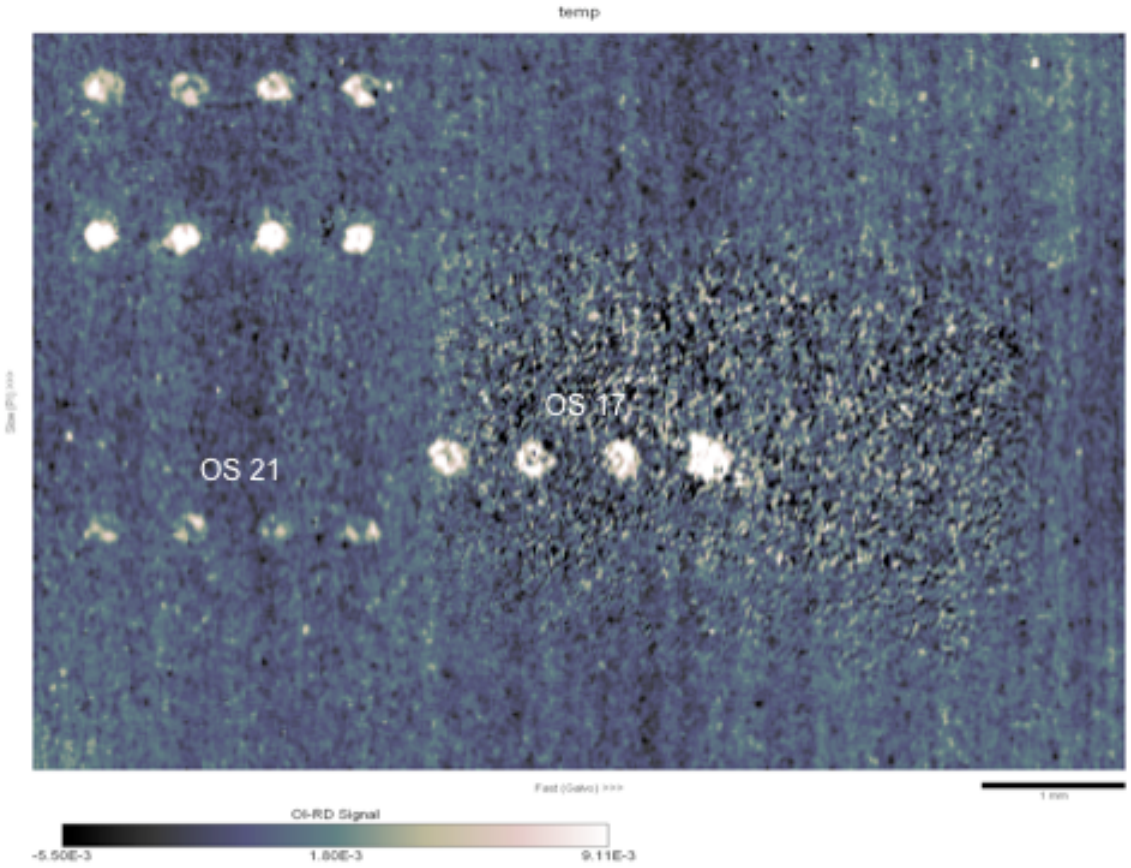

Fig. 7 120813 Difference image showing PNA (9000 nM, 1.5 hr. assoc.) binding after PR8 was flowed (5000 HAU/mL, 2 hr. assoc., .5 hr. dissoc.). Image before PBS washing.

Glycan I.D.	Glycan Structures				
OS-1		Gal	β-Biotin		
OS-2		GalNAc	α-Biotin		
OS-3		Gal	β1-4Glc	β-Biotin	
OS-4		Gal6S	β1-4Glc	β-Biotin	
OS-5		Gal	β1-4GlcNAc	β-Biotin	
OS-6		Gal	β1-4GlcNAc6S	β-Biotin	
OS-7		Gal	β1-3GlcNAc	β-Biotin	
OS-8		Gal	β1-3GlcNAc	β1-3Galβ1-4Glc	β-Biotin
OS-9		Gal	β1-3GalNAc	β-Biotin	
OS-10	Neu5Acα2-3	Gal	β-Biotin		
OS-11	Neu5Acα2-3	Gal	β1-4Glc	β-Biotin	
OS-12	Neu5Acα2-3	Gal6S	β1-4Glc	β-Biotin	
OS-13	Neu5Acα2-3	Gal	β1-4GlcNAc	β-Biotin	
OS-14	Neu5Acα2-3	Gal	β1-4GlcNAc6S	β-Biotin	
OS-15	Neu5Acα2-3	Gal	β1-3GlcNAc	β-Biotin	
OS-16	Neu5Acα2-3	Gal	β1-3GlcNAc	β1-3Galβ1-4Glc	β-Biotin
OS-17	Neu5Acα2-3	Gal	β1-3GalNAc	β-Biotin	
OS-18	Neu5Acα2-6	GalNAc	α-Biotin		
OS-19	Kdnα2-6	Gal	β1-4Glc	β-Biotin	
OS-20	Neu5Gcα2-6	Gal	β1-4Glc	β-Biotin	
OS-21	Neu5Acα2-6	Gal	β1-4Glc	β-Biotin	
OS-22	Neu5Acα2-6	Gal	β1-4GlcNAc	β-Biotin	
OS-23	Neu5Acα2-6	Gal	β1-4GlcNAc6S	β-Biotin	
OS-24	Neu5Acα2-6	Gal	β1-3GlcNAc	β-Biotin	

Table 1. List of glycans used. Far right column describes how sialic acid was bound.

Base structure	OS-1	OS-2	OS-3	OS-4	OS-5	OS-6	OS-7	OS-8	OS-9
Neu5Acα2,3	OS-10		OS-11	OS-12	OS-13	OS-14	OS-15	OS-16	OS-17
Neu5Acα2,6		OS-18	OS-21		OS-22	OS-23	OS-24		
Kdnα2,6			OS-19						
Neu5Gcα2,6			OS-20						

Table 2. A tabular formulation of glycans used in the experiment. The first row is the base structure, second is the base structure with α2,3-linked sialic acid, and the third is the base structure with α2,6-linked sialic acid.

Glycan	H1N1 MDCK-1	H1N1 MDCK-2	PR8 MDCK	PR8 Egg	Mem71 MDCK	Mem71 Egg	Phil MDCK	Phil Egg	Udorn MDCK	Udorn Egg
OS-1										
OS-2										
OS-3										
OS-4										
OS-5										
OS-6										
OS-7										
OS-8										
OS-9										
OS-10(α2,3)			Y	Y	Y	Y	Y	Y	Y	Y
OS-11(α2,3)			Y	Y	Y	Y	Y	Y	Y	Y
OS-12(α2,3)			Y	Y	Y	Y	Y	Y	Y	Y
OS-13(α2,3)			Y	Y	Y	Y	Y	Y	Y	Y
OS-14(α2,3)		Y	Y	Y	Y	Y	Y	Y	Y	Y
OS-15(α2,3)			Y	Y	Y	Y	Y	Y	Y	Y
OS-16(α2,3)			Y	Y	Y	Y	Y	Y	Y	Y
OS-17(α2,3)			Y	Y	Y	Y	Y	Y	Y	Y
OS-18(α2,6)		Y			Y	Y			Y	Y
OS-19(α2,6)										
OS-20(α2,6)									Y	Y
OS-21(α2,6)	Y	Y	Y	Y	Y	Y	Y	Y	Y	Y
OS-22(α2,6)	Y	Y	Y	Y	Y	Y	Y	Y	Y	Y
OS-23(α2,6)	Y	Y	Y	Y	Y	Y	Y	Y	Y	Y
OS-24(α2,6)	Y	Y	Y	Y	Y	Y	Y	Y	Y	Y

Note: Seasonal H1N1, MDCK-1 sample was received in May, 2011
Seasonal H1N1, MDCK-2 sample was received in Dec, 2011. **This sample was grown from sample received in May, 2011.**
Pandemic PR8, Mem71, Phil and Udorn were grown in MDCK and egg
Samples grown in MDCK were not purified
Samples grown in egg were purified

Table 3. Previous unpublished data taken by Y. Y. Fei—binding profile of HA to listed glycans for four pandemic (PR8, Mem71, Phil, and Udorn) and one seasonal strain (H1N1). MDCK refers to sample growth in MDCK medium, while egg refers to growth in egg medium. MDCK-2 refers to second generation of the seasonal virus.

Works Cited

1. Iwatsuki-Horimoto, K. et al. 2006. The cytoplasmic tail of Influenza A virus M2 protein plays a role in viral assembly. Journal of Virology 80: 5233-5240.
2. Matrosovich, M. and H.D. Klenk. 2003. Natural and synthetic sialic acid-containing inhibitors of influenza virus receptor binding. Review of Medicinal Virology 13: 85-97.
3. Wagner, R., M. Matrosovich, and H. D. Klenk. 2002. Functional balance between hemaggluninin and neuraminidase in influenza A virus infections. 12: 159-166. Review Medicinal Virology 12: 159-166.
4. Lambre, C. R., Terzidis, H., Greffard, A., and R. G. Webster. 1990. Measurement of anti-influenza neuramindase antibody using a peroxidase-linked lectin and microtitre plates coated with natural substrates. Journal of Immunology Methods 135:49-57.
5. Fei, Y. Y., J. P. Landry, Y. S. Sun, X. D. Zhu, J. T. Luo, X. B. Wang, and K. S. Lam. 2008. A novel high-throughput scanning microscope for label-free detection of protein and small-molecule chemical microarrays. Rev. Sci. Instrum. 79: 013708.
6. Wang, X., L. Heng, W. Juan, Y. Kun, L. Hui-Bin, J. Kui-Juan, Z. Yue-Liang, and Y. Guo-Zhen. 2010. Label-free and high-throughput detection of protein microarrays by oblique-incidence reflectivity difference method. Chinese Physical Letters 27: 107801.

7. Wang, X. et al. 2011. Real-time and label-free detection of biomolecular interactions by oblique-incidence reflectivity difference method. Chinese Physics Bulletin 20: 010704.
8. Fei, Y.Y. et. al. 2011. Fluorescent labeling agents change binding profiles of glycan-binding proteins. Molecular Biosystems 7: 3343-3352.
9. Fei, Y. Y. et al. 2010. Screening small-molecule compound microarrays for protein ligands without fluorescence labeling with a high-throughput scanning microscope. Journal of Biomedical Optics 15: 016018.